International Journal of Solids and Structures 47 (2010) 1952–1960

Contents lists available at ScienceDirect

International Journal of Solids and Structures

journal homepage: www.elsevier.com/locate/ijsolstr

Peeling behavior of a bio-inspired nano-film on a substrate

Z.L. Peng [a], S.H. Chen [a,*], A.K. Soh [b]

[a] LNM, Institute of Mechanics, Chinese Academy of Sciences, Beijing 100190, China
[b] Department of Mechanical Engineering, The University of Hong Kong, Hong Kong, China

ARTICLE INFO

Article history:
Received 2 November 2009
Received in revised form 1 March 2010
Available online 2 April 2010

Keywords:
Bio-inspired nano-film
Peeling model
Peeling force
Adhesion length
Peeling angle

ABSTRACT

A peeling model is proposed to analyze the peeling properties of bio-mimetic nano-films using the finite element method (FEM) and theoretical approach. The influences of the nano-film's adhesion length, thickness, elastic modulus, roughness and peeling angle on the peeling force were considered as well as the effect of the viscoelastic behavior. It has been found that the effective adhesion length, at which the peeling force attained maximum, was much smaller than the real length of nano-films; and the shear force dominated in the case of smaller peeling angles, whereas, the normal force dominated at larger peeling angles. The total peeling force decreased with an increasing peeling angle. Two limiting values of the peeling-off force can be found in the viscoelastic model, which corresponds to the smaller and larger loading rate cases. The effects of nano-film thickness and Young's modulus on peeling behaviors were also discussed. The results obtained are helpful for understanding the micro-adhesion mechanisms of biological systems, such as geckos.

1. Introduction

In the 4th century B.C., Aristotle observed the ability of geckos to "run up and down a tree in any way, even with the head downwards" (Autumn et al., 2002). However, only till recently, the micro-structures of geckos' adhesive systems and the adhesion principle were observed and discovered using advanced experimental instruments. One toe of geckos includes several lamellas which contain millions of setae. Each seta is about 30–130 μm long, 4.2 μm in diameter, and it further branches into hundreds of spatula pads through several stalks. Each pad is about 200 nm in length and width, and 5 nm in thickness. The special climbing ability of geckos is due to the van der Waals forces (Autumn et al., 2000, 2002) and possible capillary force (Huber et al., 2005a; Sun et al., 2005) between substrate and the hierarchical adhesive system, as shown in Fig. 1. Such a nanometer scale adhesive system insures intimate contact with any rough surfaces such that the accumulating molecular forces could support gecko's body weight.

Many adhesive contact mechanics models (for examples, Arzt et al., 2003; Gao et al., 2003, 2005; Hui et al., 2004; Gao and Yao, 2004; Gao et al., 2005; Glassmaker et al., 2005; Chen et al., 2008a,b, 2009a,b,c; Greiner et al., 2009; Guo and Fan, 2009) have been developed in order to explain why geckos' adhesive systems possess such a high adhesion strength. Among these studies, it has been found that the adhesion strength of the contact interface between a cylindrical fiber and a substrate was affected significantly by the size of fibers and there existed a critical size under which the interfacial adhesion strength is saturated to be the theoretical one. For example, Gao et al. (2005) modeled spatula as an elastic pillar fibril adhering on a rigid substrate, and they found that the uniform stress in contact area reached the theoretical strength as the radius of the fibril was decreased to a critical value, and that the failure of contact interface was not due to crack propagation but rupture at the theoretical strength, which is called flaw tolerance (Gao et al., 2003; Gao and Chen, 2005; Chen et al., 2008b). The adhesion properties of fibrillar structures were compared to that of a flat surface adhering on a substrate (Hui et al., 2004), and it was found that the adhesion strength of the fibrillar structure can be enhanced when the size of a single fibril was below a critical value. With a self-similar model, Yao and Gao (2006) showed that the structural hierarchy could enhance adhesion if each level of the hierarchical structure satisfied flaw tolerant adhesion.

The behavior of reversible adhesion of geckos has also stirred many interesting works (Persson and Gorb, 2003; Sitti and Fearing, 2003; Gao et al., 2005; Huber et al., 2005b; Autumn et al., 2006; Tian et al., 2006; Chen and Gao, 2007; Kim and Bhushan, 2008; Zhao et al., 2008), in which contact mechanics model was mainly used to study the macroscopic reversible mechanism. For example, Chen and Gao (2007) found that the reversible attachment and detachment was due to the anisotropic property of bio-adhesive tissues and the adhesion strength of the contact interface varied with the orientation of external loading, which has been experimentally verified by Lee et al. (2008).

* Corresponding author. Tel.: +86 10 82543960; fax: +86 10 82543977.
E-mail address: chenshaohua72@hotmail.com (S.H. Chen).

0020-7683/$ - see front matter © 2010 Elsevier Ltd. All rights reserved.
doi:10.1016/j.ijsolstr.2010.03.035

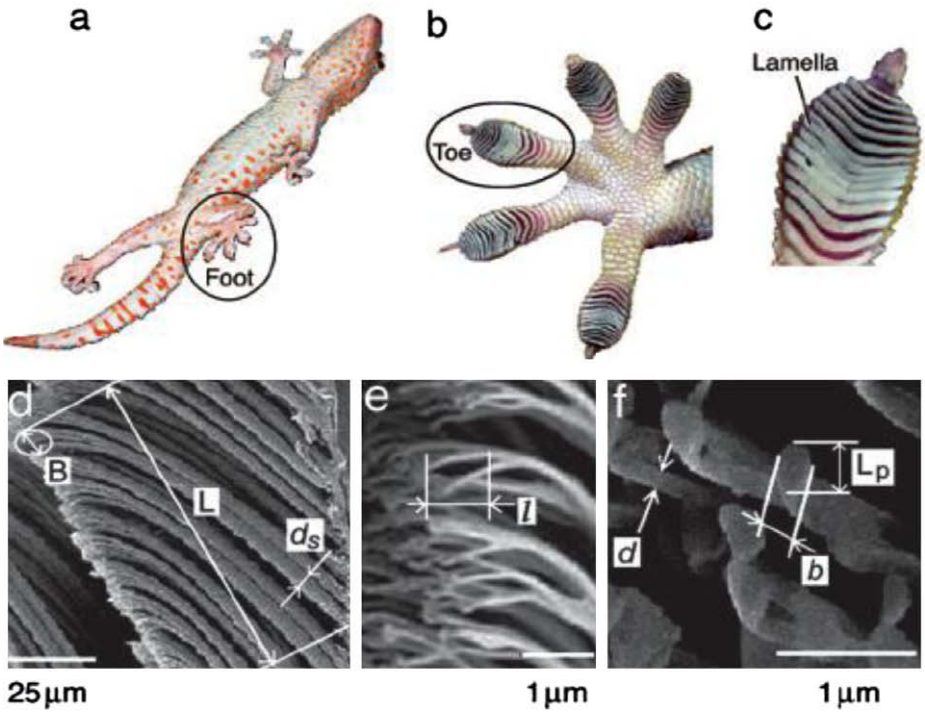

Fig. 1. Hierarchical structures of a gecko's adhesive pad: (a–f) structures shown in order of a decreasing size. (a) Gecko, (b) foot, (c) toe, (d) setal array, (e) spatulae, and (f) spatula pads. Adopted from Tian et al. (2006).

In order to enhance the bionic technology and guide the design of biomimetic adhesion structures, it is necessary and important to investigate microscopic adhesion behaviors and microscopic reversible mechanisms. It is known that the real profile of the smallest element (spatula) in geckos' pad looks like a nano-film with finite scales. Experimental observations have shown that the mechanical behavior of a spatulae is detaching from a substrate under a peeling force. However, in most of the existing contact models, the pulling force considered can be very useful for determining the macroscopic adhesion and reversible mechanisms but not the microscopic mechanism, which plays a dominant role when micro-structures and loading patterns of geckos' nano-film-like spatula are involved. Chen et al. (2009a) used a Kendall's peeling model to show that the peeling force of a spatula could varied significantly with the peeling angle by modeling the adhesion behavior of a spatula as an elastic tape adhering on a rigid substrate. Tian et al. (2006) obtained the peeling force as a function of the peeling angle based on a frictional adhesion model, in which the mechanism of reversible adhesion was explained by assuming that the number of spatulae contacting with a substrate is much larger during attachment than that of detachment. Similar to the famous Kendall's model, in these biomimetic peeling models, the adhesion length of the nano-film was assumed to be infinite (Chen et al., 2009a) or taken from the experimental observations directly (Tian et al., 2006), and the influence of adhesion length on the maximum peeling force (Peeling-off force) was not considered. In 2007, Pesika, et al. considered a length term in their peel-zone model, but they did not focus on how the adhesion length influenced the adhesion properties.

In the present study, a peeling model of a nano-film in adhesive contact with a substrate under a peeling force is established, in which the nano-film has a finite adhesion length similar to geckos' spatulae. Influences of the nano-films' adhesion length and peeling angle on the peeling force are mainly considered numerically and theoretically. The results obtained from the present study should be helpful for understanding the micro-adhesion mechanisms of biological systems.

2. Numerical model

As mentioned above, a single spatula of geckos consists of a shaft and a pad. Each spatula pad looks like a nano-film with finite scales, i.e., about 200 nm in length and width, and 5 nm in thickness. A plane strain numerical model is established as shown in Fig. 2, in which a nano-film with length L, subjected to an external peeling force P, contacts adhesively with a rigid substrate. The film thickness is t and the peeling angle is θ.

Although the behavior of a spatula was investigated by Chen et al. (2009a), the spatula pad was taken as a Kendall elastic tape with infinite adhesion length. Gao and Chen (2005) have shown that the flaw tolerant interfacial strength can be achieved when the dimension of a structure was reduced to a critical length. This finding should be very useful for the future man-made high-strength materials and bio-technologies. The question is whether the length of geckos' adhesive pads is helpful for realizing flaw tolerant adhesion. If the length is larger than the critical value for flaw tolerance, why do geckos overbuild it? This study will try to answer both questions.

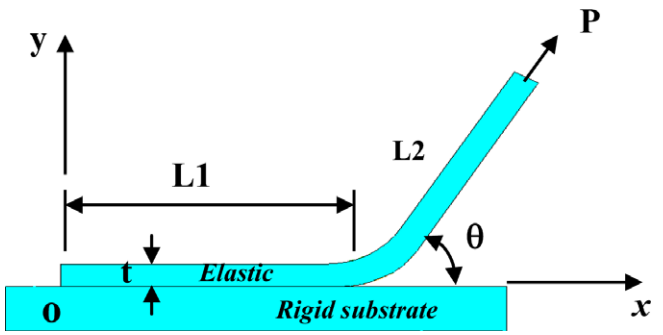

Fig. 2. Peeling model of an elastic nano-film with thickness t and adhesion length L in contact with a rigid substrate, in which P is the peeling force and θ is the peeling angle.

Numerical simulation is carried out based on the code developed by Dr. Patrick Klein of Sandia National Laboratory (http://tahoe.ca.sandia.gov). The nano-film is assumed to be elastic with Young's modulus E=2 GPa. 4-noded plane strain elements modified by Simo and Taylor are chosen to devise the model in order to improve the performance of bending and the nearly incompressible state of deformation. The molecular interaction between the two contact surfaces is represented by a layer of cohesive elements. In the following simulations, the length of nano-film L is assumed to be 50 nm.

The constitutive relation of cohesive surface elements was developed by Tvergaard and Hutchinson (1996). Other cohesive models (Barenblatt, 1959; Rahulkumar et al., 2000; Rose et al., 1981; Willis, 1967; Xu and Needleman, 1994) could in principle also be used to model molecular adhesion. However, the Tvergaard–Hutchinson model is chosen in the present study because it preserves the van der Waals energy regardless of the peeling orientation. Whereas, other cohesive models with various consideration of tension versus shear dominated separation do not necessarily preserve the interaction energy (Gao et al., 2005). The thickness of cohesive surface element is zero initially and the interaction vanishes, which represents the equilibrium state of competition between repulsion and attraction of molecular interaction. The two adhesive surfaces separate each other under a peeling force, which results in an attraction force, as shown in Fig. 3a and b.

The interfacial interaction potential in Tvergaard–Hutchinson is defined as

$$\Pi(\delta_n,\delta_t)=\delta_n^c\int_0^{\lambda}\phi(\tilde{\lambda})d\tilde{\lambda} \tag{1}$$

where λ denotes dimensionless interfacial separation,

$$\lambda=\sqrt{\left(\frac{\delta_n}{\delta_n^c}\right)^2+\left(\frac{\delta_t}{\delta_t^c}\right)^2} \tag{2}$$

where δ_n and δ_t are the normal and tangential displacement components of the separating interface, respectively; δ_n^c and δ_t^c are the corresponding critical values of the displacement components. Complete separation will happen and the interfacial tractions drop to zero when $\lambda=1$.

The force function ϕ is taken to be tri-linear,

$$\phi(\lambda)=\begin{cases}\sigma_0\lambda/\lambda_1, & (0<\lambda<\lambda_1)\\ \sigma_0, & (\lambda_1<\lambda_1<\lambda_2)\\ \sigma_0(1-\lambda)/(1-\lambda_2), & (\lambda_2<\lambda<1)\end{cases} \tag{3}$$

which is shown schematically in Fig. 3 (c).

The normal and tangential tractions in cohesive zone are given by

$$T_n=\frac{\partial\prod}{\partial\delta_n}=\frac{\phi(\lambda)}{\lambda}\frac{\delta_n}{\delta_n^c},\quad T_t=\frac{\partial\prod}{\partial\delta_t}=\frac{\phi(\lambda)}{\lambda}\frac{\delta_t}{\delta_t^c}\frac{\delta_n^c}{\delta_t^c} \tag{4}$$

The Tvergaard–Hutchinson law takes into account both normal and tangential tractions with a constant work of adhesion,

$$\Gamma_0=\frac{1}{2}\sigma_0\delta_n^c[1-\lambda_1+\lambda_2] \tag{5}$$

According to Wei (2004), the numerical results, at least the variation trends of the results are insensitive to the values of λ_1 and λ_2, so the values of λ_1 and λ_2 are taken as

$$\lambda_1=0.001,\quad \lambda_2=0.999 \tag{6}$$

Values of the other material constants are taken from Gao et al. (2005), in which the flaw tolerant adhesion of geckos' seta were discussed.

$$\begin{cases}\sigma_0=20\ \text{MPa}, & \Gamma_0=0.01\ \text{J/m}^2\\ \delta_n^c=\delta_t^c=0.5\ \text{nm}, & E=2\ \text{GPa}\end{cases} \tag{7}$$

One should be noted that the work of adhesion defined in Eq. (5) is a constant. In fact, it is known that the interfacial fracture toughness, defined here as the work of adhesion, can have a strong dependence on the mode of failure through the mode-mixity angle $\psi=\tan^{-1}(K_2/K_1)$ as (Evans et al., 1990; Thouless and Jensen, 1992; Hutchinson and Suo, 1992)

$$\Gamma(\theta)=\Gamma_0/(1-\lambda\sin^2\psi) \tag{8}$$

where K_1 and K_2 denote the modes I and II stress intensity factors, respectively. ψ depends on the peeling angle θ as shown in Chen et al. (2009a) and λ is a parameter ranging from 0 to 1. The work of adhesion is a constant independent of the mode mixity angle ψ when $\lambda=0$ and becomes increasingly dependent on ψ as λ increases toward 1 as discussed in Chen et al. (2009a).

It is found that the effect of mode-mixity can enhance the interfacial adhesion strength at low peeling angles, however the results in the case of a mode-mixity dependent work of adhesion are qualitatively similar to that in the case of a constant work of adhesion (Chen et al., 2009a). In the present adhesive contact model, we assume that the work of adhesion is a constant independent of the local failure mode.

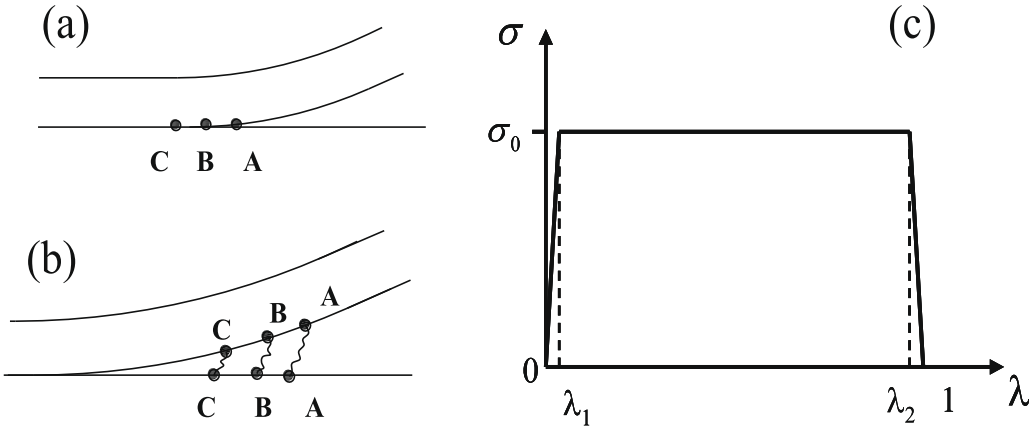

Fig. 3. Schematic of the cohesive interface and constitutive relation of cohesive element. (a) Before separation, (b) adhesive interface separation, (c) constitutive relation of a cohesive element.

3. Numerical results and discussions

3.1. The effect of adhesion length

The effect of the effective adhesion length of nano-films on the peeling force is investigated in this sub-section. It is a known fact that there exists a critical size of an elastic cylindrical punch in adhesive contact with a rigid substrate, below which the adhesion strength of the contact interface is saturated to be the theoretical one (Gao et al., 2005). Is there such a phenomenon in the present model of nano-film adhesion?

For a nano-film with length 50 nm, Fig. 4 (a) clearly indicates that, at the moment of peeling-off, the interfacial tractions in part of the adhesion length are saturated to be the theoretical interfacial strength (we call this part as saturation adhesion length or effective adhesion length), while those in another part of the adhesion length is smaller than the theoretical one. It is found that the peeling angle influences the saturation length of interfacial traction significantly. The saturation adhesion length as well as the peeling-off force decreases with increasing peeling angle. The peeling-off force under a determined peeling angle will keep a constant only if the adhesion length is larger than the saturation one.

The saturation adhesion lengths for the case of varying peeling angle are shown in Fig. 4 (b). One can clearly see that the saturation adhesion length decreases with an increasing peeling angle. However, even the longest saturation size is much smaller than the real length of a spatula pad of 200 nm. For example, the saturation adhesion lengths are about 25 nm and 7 nm when the peeling angles are 0° and 90°, respectively. It is very obvious that the saturation size in the present peeling model is much smaller than the critical size for flaw tolerant adhesion in a tension model (Gao et al., 2005). It can be inferred that the whole length of geckos' spatula, i.e., 200 nm, is not designed to achieve flaw tolerant adhesion under peeling behavior.

Fig. 4 (c) shows the dimensionless peeling-off force as a function of the adhesion length for different peeling angles. From Fig. 4(c), one can see that when the film length is smaller than the saturation adhesion length, the cohesive zone length that essentially bears the peeling force equals to the whole film length. The peeling-off force will increase along with an increasing adhesion length and keeps a constant when the adhesion length attains the saturation one.

The question is why geckos overbuild the length of a spatula pad. It is a known fact that surfaces in nature cannot be perfectly smooth and have different roughness. The area of intimate adhesion will be reduced due to the surface roughness, which will decrease the adhesion force. Persson and his collaborators have done a lot of excellent researches about the effect of roughness on adhesion (Persson and Gorb, 2003; Persson, 2003). In the present study, a very simple adhesion–peeling model will be used to analyze the combined effect of roughness and effective adhesion length on peeling-off force in the following section.

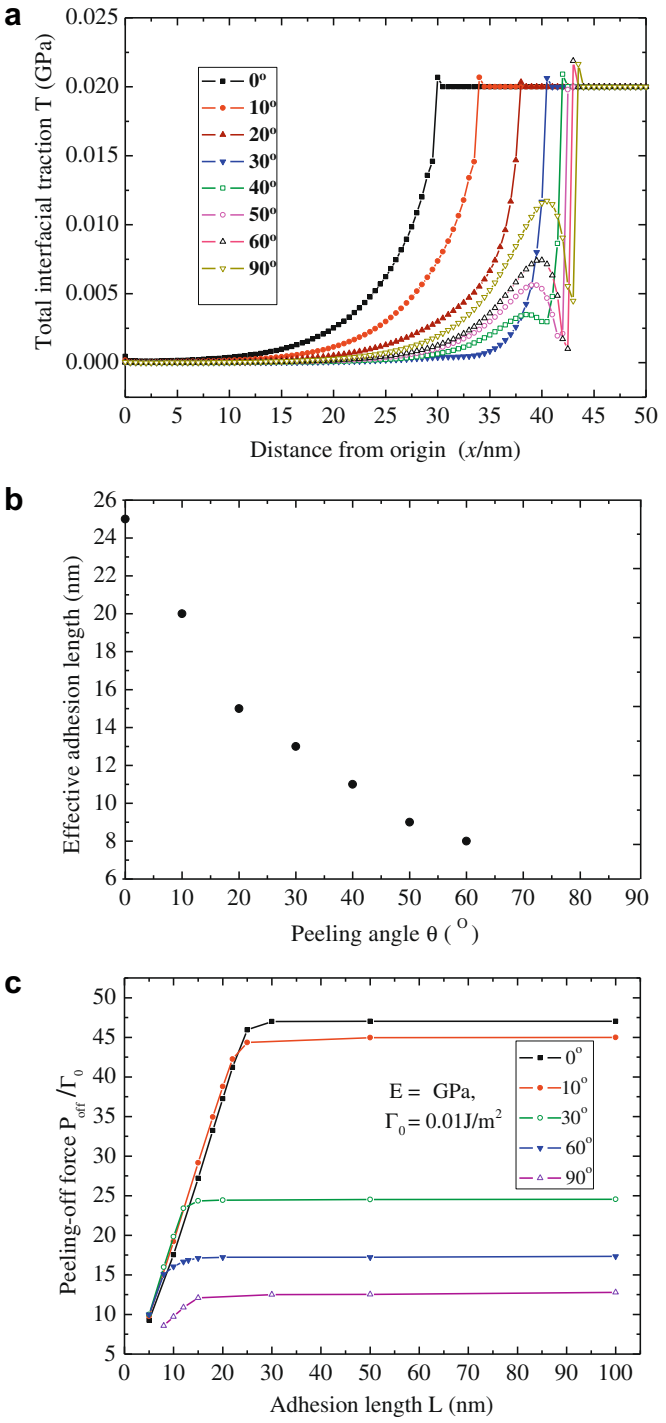

Fig. 4. (a) Distributions of the total interfacial traction T for nano-film along the adhesive interface for the cases with different peeling angles. (b) Effective adhesion length L_{cr} for the cases with various peeling angles θ. (c) Dimensionless peeling-off force as a function of the adhesion length with various peeling angles.

3.2. Effect of the peeling angle on adhesion behavior

The effect of the peeling angle on the peeling-off force is shown in Fig. 5, in which the peeling angle shows significant influences not only on the peeling-off force but also its normal and tangential components. When the peeling angle is near a tangential direction of the contact interface, i.e., 0°, the normal component of the peeling-off force vanishes and the tangential component equals to the total peeling-off force. When the peeling angle is increased, the normal component of the peeling-off force increases first and then keeps almost a constant when the peeling angle is larger than 30°, which agrees well with the conclusions of a peel-zone model proposed by Pesika et al. (2007). The peel-zone model (Pesika et al., 2007) is different from the Kendall one by an angle-dependent multiplier, which takes into account the increase in the length of the peel zone when the peel angle is reduced. Furthermore, in their PZ model, Pesika et al. find an experimentally determined critical angle beyond which the shape and dimension of the peeling-zone remains a constant, thus the normal component of the peeling-off force also remains constant. The critical angle, as an intrinsic property of the tape backing, adhesive, and substrate system, is

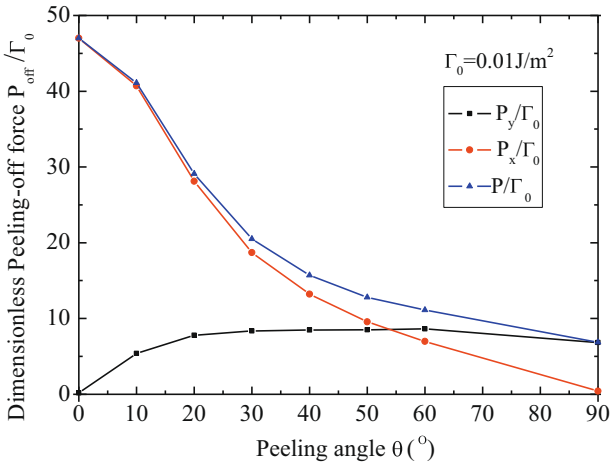

Fig. 5. Effect of the peeling angle θ on the dimensionless peeling-off force P_{off}/Γ_0 and its normal and tangential components.

dependent of the tackiness of the adhesive. In other words, the material constants taken in our present peeling model corresponds to one kind of adhesives analyzed by Pesika et al. (2007). On the other hand, when the peeling angle is smaller than 30°, the tangential force is the main contributor for the total peeling-off force. This result tallies well with the findings in a frictional adhesion model proposed by Tian et al. (2006). In a whole, the results should be helpful for understanding how geckos adhere on vertical walls or ceilings. A much larger tangential component exists in most cases may help to explain why geckos tend to spend more time on walls instead of ceilings.

3.3. Peeling-off force of a two-spatulae structure

Experimental measurements show that each spatula of geckos supports the peeling-off force by almost equal amount (Huber et al., 2005a; Hui et al., 2004), which is called equal load sharing (ELS). ELS is also examined by our peeling model using two identical nano-films, as shown in the inset of Fig. 6, from which one can see that the shape of the peeling model is non-symmetric. However, the results presented in Fig. 6 demonstrate that the peeling-off force of the combined asymmetric structure equals almost two times that of the peeling-off force of a single spatula

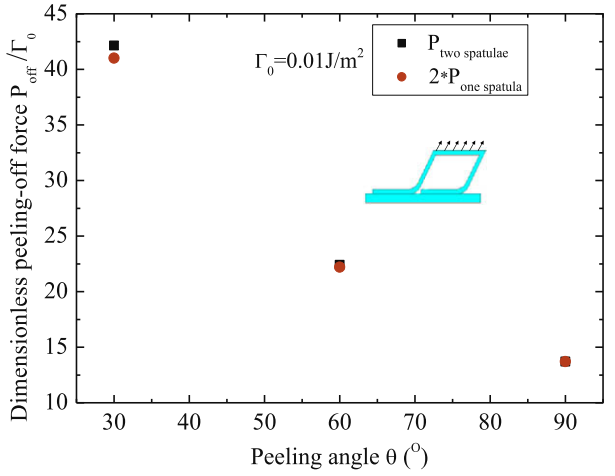

Fig. 6. The dimensionless peeling-off force P_{off}/Γ_0 for the combined spatulae structure to demonstrate equal load sharing under different peeling angles θ.

for different peeling angle cases. At a first glance, it may seem intuitive that the results of Fig. 6 are obvious. Actually, one should note that the combined structure is asymmetric, which causes the external peeling force asymmetric. For a symmetric fibrillar array structure, the ELS condition can be satisfied only when the adhesion of each fiber is flaw tolerant, otherwise, the fibrils near the periphery of fibrillar structure will detach first (Hui et al., 2004). While in our peeling model, it has been shown in the above subsection that flaw tolerance cannot be satisfied but the ELS condition is still met. For a living gecko, it has been demonstrated that rolling in or rolling out of gecko's toe can lead to clockwise directional moment or counter-clockwise directional moment on seta shaft, which can lead to different peeling angles on spatulae structure. Through this kind of function, gecko can achieve different peeling-off force to realize attachment and detachment. During the reversible adhesion, each spatula has an identical peeling-off force, at least on a perfect smooth surface.

3.4. Effect of surface roughness on peeling behavior

Natural surfaces, including highly polished surfaces, have roughness in many different length scales. Surface roughness has a great influence on adhesion between solids (Persson and Gorb, 2003). In order to study the effect of the surface roughness on spatula-peeling behavior, we simulate the surface roughness as a weak adhesion zone or a crack with a finite size similar to Gao et al. (2005) as shown in Fig. 7(a), in which the crack length is taken to be 5, 10, 15, and 20 nm. The effect of cracks with different lengths, is shown in Fig. 7(b). It is obvious that the peeling-off force remains constant with increasing crack length. However, experimental observations demonstrate that even a small scale surface roughness can decrease adhesion severely in the system of an elastic ball adhering on a rough substrate (Briggs and Briscoe, 1977; Fuller and Tabor, 1975). The real contact area is reduced due to the surface roughness. In the present peeling model, one can see

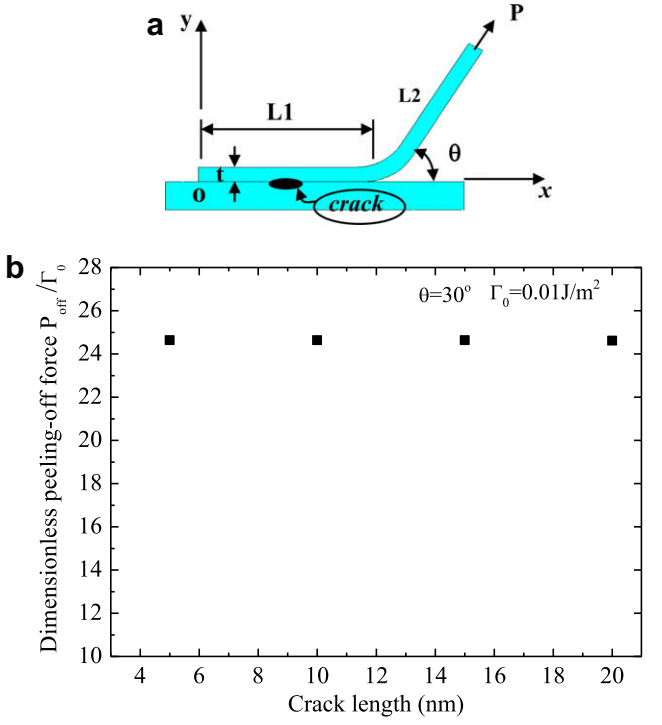

Fig. 7. (a) A crack model to describe the effect of the surface roughness on the peeling-off force P_{off}. (b) The effect of crack length on the dimensionless peeling-off force P_{off}/Γ_0 at a peeling angle of 30°.

that the effective adhesion length is not larger than the whole adhesive length as shown in Fig. 4(c). If the film length is not less than the effective adhesion length (saturation length), the peeling-off force will keep the maximum (platform value in Fig. 4(c)) and be insensitive to the crack length. Otherwise, the peeling-off force can be found in the initial increasing phase in Fig. 4(c). As for a more interesting model to consider a periodic array of weak zones within the adhesion region, Chen et al. (2008a) has used such a kind model and shown that the critical peeling force is almost a constant in explaining ssDNA adhering on graphite substrate. From Chen et al. (2008a), we can infer the peeling-off force should keep a constant only if the subdivision adhesion length is identical in a periodic crack model for the present problem. The value of the peeling-off force also corresponds to the subdivision adhesion length as shown in Fig. 4(c) if it is not larger than the saturation length. Otherwise, the peeling-off force will achieve the maximum.

Although the model to simulate the effect of surface roughness is very simple, the results can still reveal qualitatively that the peeling-off force is independent of the crack length only if the crack length is not larger than the difference of the entire adhesion length and the effective length found in Section 3.1. This result may help to partly explain why geckos overbuild the length of a spatula (about 200 nm). The overbuilt length can be used to adapt to surfaces with different roughness. For the case of larger surface roughness, nano-films may adopt the real shape of the surface roughness to increase adhesion area (Persson and Gorb, 2003).

3.5. Effects of Young's modulus and thickness of nano-films

In recent years, peeling tests become popular because they are the convenient and simple way to measure interfacial strength or adhesion. The mechanical behavior of gecko's spatula is similar to a nano-film adhering on a substrate. It should be useful to understand the effect of Young's modulus and the thickness of nano-films on peeling actions.

Fig. 8(a) and (b) present the effects of the thickness and Young's modulus of nano-films, respectively, on interfacial tractions with peeling angle equals to 30°. It is found that the thickness and Young's modulus significantly influence the effective length of interfacial traction distribution as well as the saturation length, at which the interfacial traction attains the theoretical interfacial strength. Both the effective adhesion length and the saturation length increase with increasing thickness and Young's modulus of nano-films. It is a known fact that the bending and axial stiffness of nano-films increase with increasing thickness and Young's modulus such that a greater part of the applied force is transferred to the film away from the loaded end. The results obtained agree well with those found for micro- and macro-scale films (De Lorenzis and Zavarise, 2008; Yuan et al., 2007). However, these results can only be applied to a perfect contact between a thin film and a smooth substrate. For the case of rough substrate, this conclusion may not be reasonable. For a thicker film to contact intimately with a rough substrate, it needs a lot of film-bending energy. In this case, an effective interface energy Γ_{eff} should be defined to replace the surface energy Γ_0 of a smooth surface as in Persson (2003) and Persson and Gorb (2003). The effective interface energy can be written

$$\Gamma_{eff} = \Gamma_0 - U_{el} \tag{9}$$

where U_{el} is the elastic energy in order to make atomic contact at the interface. From the above equation, it demonstrates that much elastic energy stored in the film can reduce effective interface energy greatly. If $U_{el} = \Gamma_0$, the effective interface energy Γ_{eff} becomes zero, and the film cannot adhere on the substrate. So for the case with a rough substrate, a thinner film can not only makes intimate contact easily at the interface but increase the effective interface

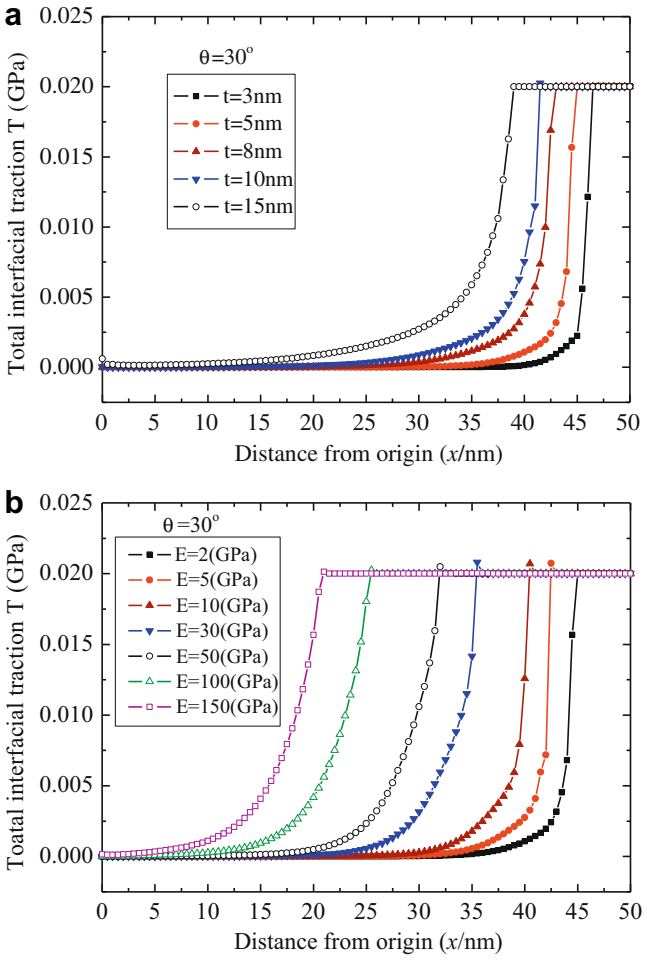

Fig. 8. Distribution of the total interfacial traction T for the cases of various nano-films at a fixed peeling angle 30°. (a) Nano-films with different thickness (b) Nano-films with different Young's moduli.

energy due to a small stiffness and less elastic energy stored for bending. The thin spatula thickness that geckos adopt may also be an appropriate one so that geckos can achieve intimate contact with rough surface and attain necessary adhesion force.

As for the details that why geckos possess spatulae with 5 nm thickness, the issue may be discussed later based on the effective molecular interaction distance between two surfaces (Israelachvili, 1992; Israelachvili and Tabor, 1972).

3.6. Effect of viscoelastic behavior of the film on the peeling-off force

As we know that most of the biological materials are viscoelastic. For simplicity, most literatures have assumed the biomimetic material to be elastic. Here, in order to analyze the effect of viscoelastic behavior of the film on the peeling force, we adopt an ordinary linear viscoelastic law similar to Chen et al. (2010) to describe the nano-film,

$$\mu(t) = \mu_\infty + \mu_{neq} \exp(-t/\tau_s) \tag{10}$$

where μ is the shear modulus varying with time t. τ_s is the relaxation time of shear modulus. The bulk modulus is always assumed to be a constant and Poisson's ratio be 0.25. According to Russell (1975) and Chen et al. (2010), we take $\tau_s = 2$ ms. Both the relaxed shear moduli μ_∞ and μ_{neq} are taken as 0.8 GPa, which results in a varying relaxed Young's modulus $E(t)$ during the whole relaxation process with the instantaneous relaxed Young's modulus 3.43 GPa

and the relaxed Young's modulus 2 GPa, which is identical to the Young's modulus of a gecko's spatula (Gao et al., 2005). One should be noted that other viscoelastic laws can also be used to find the effect of visco-elasticity on adhesion.

Fig. 9 shows the dimensionless peeling force as a function of loading rate at different peeling angles. It is found that the peeling force varies significantly with the loading rate at a small peeling angle, while it keeps almost a constant with an increasing loading rate at large peeling angle, for example, 90°. For the case with a determined peeling angle, the peeling force tends to be a limiting value at a smaller and a larger loading rate, respectively. The two limiting values of the peeling force at a smaller or larger loading rate are consistent with the ones in the elastic models with the instantaneous relaxed Young's modulus 3.43 GPa and the relaxed Young's modulus 2 GPa. From above that geckos tends to attach on a surface with a small peeling angle and detach at a large peeling angle, it can be inferred that the viscoelastic property of a spatula is more beneficial for gecko to achieve robust attachment and easy detachment.

4. Theoretical analysis

4.1. The effect of adhesion length

There are very few theoretical models that consider the effect of adhesion length of nano-films on the peeling behavior. It can be found in the numerical simulation section that not the whole film length but an effective adhesion length withstands the external peeling force. The effective adhesion length can be divided into two parts according to the interfacial tractions, in which a saturation length is defined according to the saturating interfacial tractions. In order to predict the saturation length theoretically, a simple model is established, as shown in Fig. 10. For simplicity, the effective adhesion length is assumed to be approximately identical to the saturation length, which is denoted as L_c in Fig. 10. Later, a more realistic model would be established in our future work. Assuming the geometry of peeling-off part near the substrate as a circular shape with radius R and arc length L_R. p is a peeling force acting at the end of the nano-film.

It is reasonable to assume the molecular interaction between the nano-film and substrate as that described by the Tvergaard–Hutchinson model, as shown in Fig. 3 (c), in which σ_0 is a resultant force that differs from the normal one in the Dugdale model.

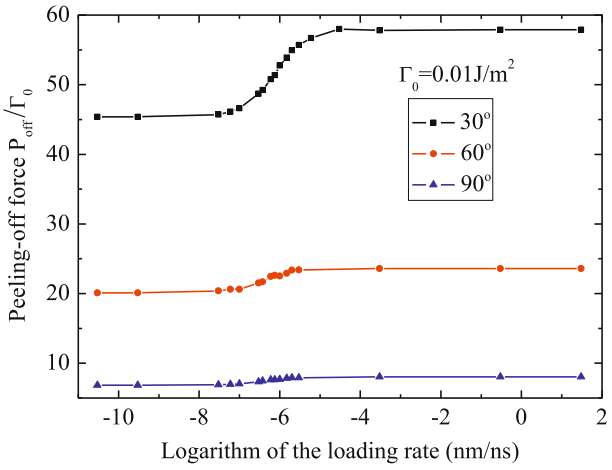

Fig. 9. Dimensionless peeling-off force as a function of the loading rate for the viscoelastic nano-film case.

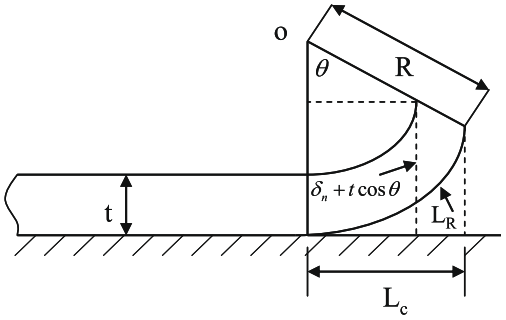

Fig. 10. Schematic of the effective peeling-zone.

Before the propagation of peeling-zone, the energy balance among the strain energy, the work of the peeling force and the adhesion energy can be expressed as

$$\int_0^{L_c} \sigma_0 \delta_n^c \frac{R-\sqrt{R^2-x^2}}{R}dx = \frac{1}{2}p\cdot t\cdot(L_R-L_c) - \frac{1}{2}E\cdot\varepsilon^2\cdot L_R\cdot t \tag{11}$$

where the elastic strain of the nano-film is denoted as $\varepsilon = p/E$, E is the Young's modulus. The arc length is denoted as $L_R = R\theta$, where θ is the peeling angle. For the case of small peeling angle, we have

$$R = \frac{\delta_n}{1-\cos\theta} \tag{12}$$

where δ_n is the normal separation of the contact interface. However, Eq. (12) will be invalid for the case of large peeling angle. Instead, we approximately compute the radius of the peeling-zone as

$$R = \frac{\delta_n + t\cos\theta}{1-\cos\theta} + t \tag{13}$$

Eq. (13) agrees approximately with the empirical power-law relation used by Tian et al. (2006), $R = 4215\times\theta^{-1.35}$ (nm). Due to the above assumption that the effective adhesion length is represented by the saturation length, then we have

$$p\cdot t = \sigma_0\cdot L_c \tag{14}$$

Eqs. (11)–(14) yields the effective adhesion length L_c as

$$\Gamma_0\left\{L_c - \frac{R}{2}\left[\arcsin\frac{L_c}{R} + \frac{1}{2}\sin\left(2\arcsin\frac{L_c}{R}\right)\right]\right\} = \frac{1}{2}p\cdot t\cdot(L_R-L_c) - \frac{1}{2}E\cdot\varepsilon^2\cdot L_R\cdot t \tag{15}$$

Table 1 gives the effective adhesion length predicted theoretically by Eq. (15), which is compared with those obtained by numerical calculations. From Table 1, one can see that both predictions have the same variation trend and the same order of magnitude. Some obvious deviations exist between the numerical and theoretical predictions. There are several reasons that cause the deviations. First, in the theoretical model, we have adopted the assumption that the saturation length represents the effective length. In fact, the effective length consists of not only the saturation length but also the part in which the interfacial tractions are less than the theoretical interfacial strength. Second, the assumption of circular shape of the peeling-zone and the bending energy is not included

Table 1
Comparison of the saturation adhesion length predicted by the theoretical model and the numerical calculation.

Peeling angle (θ)	10°	20°	30°	40°	50°	60°	90°
$L_{Saturation}$(Theoretical) (nm)	37	28	19	16	12	10	8
$L_{Saturation}$ (Numerical) (nm)	20	15	13	11	9	8	7

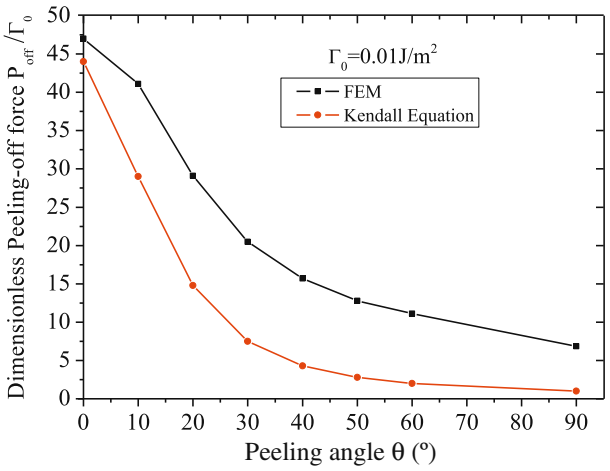

Fig. 11. Comparison of the dimensionless peeling-off force P_{off}/Γ_0 as a function of the peeling angle θ in the present numerical model and Kendall's model.

in the equilibrium of energy balance. Generally speaking, the present theoretical model is approximately valid to predict the order of magnitude of the effective adhesion length, beyond which the nano-film will be peeled off from the rigid substrate.

4.2. Comparison with Kendall's model

Kendall's peeling model (Kendall, 1975) is very popular in studying the mechanical behavior of film-substrate interface, in which it is assumed that the adhesion length of film is infinite. According to Kendall's model, the peeling force can be expressed as a function of the peeling angle,

$$p = \frac{2\Gamma_0}{\sqrt{(1-\cos\theta)^2 + \frac{2\Gamma_0}{Et}} + (1-\cos\theta)} \tag{16}$$

where p is the peeling force, Γ_0 is the fracture energy required per unit area of the interface. The peeling force as a function of the peeling angle in Kendall's model and the present numerical simulation model is shown in Fig. 11, which shows that the variation tendency of our numerical results is consistent with that predicted by Kendall's model, though the numerical results of the present model with finite adhesion length is generally larger than that predicted by Kendall's model at a given peeling angle. The discrepancy may be due to the employment of different interfacial constitutive relations. In Kendall's peeling model, Griffith energy balance criterion is adopted since the failure of adhesion interface is due to interfacial crack propagation, while the Tvergaard–Hutchinson cohesive law is adopted in the present model.

5. Conclusion

A numerical peeling model for nano-films with a finite length in adhesive contact with a rigid substrate is investigated. It is found that at a given peeling angle, the peeling-off force remains constant if the length of the nano-film is larger than an effective adhesive length. Overbuilding of length in geckos' spatulae may be due to the need to overcome surface roughness. The tangential component of the peeling-off force dominates at smaller peeling angle and the normal component dominates at larger peeling angle. The peeling-off force decreases with increasing peeling angle. Furthermore, it is found that the interfacial tractions as well as the effective adhesion length increase with increasing thickness and Young's modulus of nano-films. The viscoelastic property of a spatula should be more beneficial for gecko to achieve robust attachment and easy detachment.

The saturation length predicted by a corresponding theoretical model agrees with those calculated by numerical simulations, at least in the order of the magnitude of the effective length. Comparison with the Kendall's model and the frictional adhesion model (Tian et al., 2006) shows a similar trend for the variation of peeling-off force with the peeling angle. In contrast to the PZ model, the normal component of the peeling-off force in the present paper almost keeps a constant after a critical peeling angle, which agrees well with the experimental findings in Pesika et al. (2007).

Acknowledgments

The work reported here is supported by NSFC through Grants #10972220, #10732050, and #10721202, the key project of CAS through Grant KJCX2-YW-M04.

References

Arzt, E., Gorb, S., Spolenak, R., 2003. From micro to nano contacts in biological attachment devices. Proc. Natl. Acad. Sci. USA 100, 10603–10606.
Autumn, K., Liang, Y.A., Hsieh, S.T., Zesch, W., Chan, W.P., Kenny, T.W., Fearing, R., Full, R.J., 2000. Adhesive force of a single gecko foot-hair. Nature 405, 681–685.
Autumn, K., Sitti, M., Liang, Y.C.A., Peattie, A.M., Hansen, W.R., Sponberg, S., Kenny, T.W., Fearing, R., Israelachvili, J.N., Full, R.J., 2002. Evidence for van der Waals adhesion in gecko setae. Proc. Natl. Acad. Sci. USA 99, 12252–12256.
Autumn, K., Dittmore, A., Santos, D., Spenko, M., Cutkosky, M., 2006. Frictional adhesion: a new angle on gecko attachment. J. Exp. Biol. 209, 3569–3579.
Barenblatt, G.I., 1959. Equilibrium cracks formed on a brittle fracture. Dokl. Akad. Nauk SSSR 127, 47–50.
Briggs, G.A.D., Briscoe, B.J., 1977. Effect of surface-topography on adhesion of elastic solids. J. Phys. D: Appl. Phys. 10, 2453–2466.
Chen, S.H., Gao, H.J., 2007. Bio-inspired mechanics of reversible adhesion: orientation-dependent adhesion strength for non-slipping adhesive contact with transversely isotropic elastic materials. J. Mech. Phys. Solids 55, 1001–1015.
Chen, B., Shi, X.H., Gao, H., 2008a. Apparent fracture/adhesion energy of interfaces with periodic cohesive interactions. Proc. R. Soc. A464, 657–671.
Chen, S.H., Xu, G., Soh, A.K., 2008b. Robust nanoadhesion under torque. Tribol. Lett. 29, 235–239.
Chen, B., Wu, P.D., Gao, H., 2009a. Pre-tension generates strongly reversible adhesion of a spatula pad on substrate. J. R. Soc. Interface 35, 529–537.
Chen, S.H., Yan, C., Zhang, P., Gao, H., 2009b. Mechanics of adhesive contact on a power-law elastic half-space. J. Mech. Phys. Solids 57, 1434–1448.
Chen, S.H., Yan, C., Soh, A., 2009c. Adhesive behavior of two-dimensional power-law graded materials. Int. J. Solids Struct. 46, 3398–3404.
Chen, S.H., Xu, G., Soh, A., 2010. Size-dependent adhesion strength of a single viscoelastic fiber. Tribol. Lett. 37, 375–379.
De Lorenzis, L., Zavarise, G., 2008. Modeling of mixed-mode debonding in the peel test applied to superficial reinforcements. Int. J. Solids Struct. 45, 5419–5436.
Evans, A.G., Ruhle, M., Dalgleish, B.J., Charalambides, P.G., 1990. The fracture energy of bimaterial interface. Mater. Sci. Eng. A 126, 53–64.
Fuller, K.N.G., Tabor, D., 1975. Effect of surface-roughness on adhesion of elastic solids. Proc. R. Soc. A 345, 327–342.
Gao, H.J., Chen, S.H., 2005. Flaw tolerance in a thin strip under tension. J. Appl. Mech. 72, 732–737.
Gao, H.J., Yao, H.M., 2004. Shape insensitive optimal adhesion of nanoscale fibrillar structures. Proc. Natl. Acad. Sci. USA 101, 7851–7856.
Gao, H.J., Ji, B.H., Jager, I.L., Arzt, E., Fratzl, P., 2003. Materials become insensitive to flaws at nanoscale: lessons from nature. Proc. Natl. Acad. Sci. USA 100, 5597–5600.
Gao, H.J., Wang, X., Yao, H.M., Gorb, S., Arzt, E., 2005. Mechanics of hierarchical adhesion structures of geckos. Mech. Mater. 37, 275–285.
Glassmaker, N.J., Jagota, A., Hui, C.Y., 2005. Adhesion enhancement in a biomimetic fibrillar interface. Acta Biomater. 1, 367–375.
Greiner, C., Spolenak, R., Arzta, E., 2009. Adhesion design maps for fibrillar adhesives: the effect of shape. Acta Biomater. 5, 597–606.
Guo, X., Fan, J., 2009. A generalized JKR model for two-dimensional adhesive contact of transversely isotropic piezoelectric half space. Int. J. Solids Struct. 46, 3607–3619.
Huber, G., Mantz, H., Spolenak, R., Mecke, K., Jacobs, K., Gorb, S.N., Arzt, E., 2005a. Evidence for capillarity contributions to gecko adhesion from single spatula nanomechanical measurements. Proc. Natl. Acad. Sci. USA 102, 16293–16296.
Huber, G., Gorb, S.N., Spolenak, R., Arzt, E., 2005b. Resolving the nanoscale adhesion of individual gecko spatulae by atomic force microscopy. Biol. Lett. 1, 2–4.
Hui, C.Y., Glassmaker, N.J., Tang, T., Jagota, A., 2004. Design of biomimetic fibrillar interfaces: 2. Mechanics of enhanced adhesion. J. R. Soc. Interface 1, 35–48.
Hutchinson, J.W., Suo, Z., 1992. Mixed mode cracking in layered materials. Adv. Appl. Mech. 29, 63–191.

Israelachvili, J.N., 1992. Intermolecular and Surface Forces. Academic Press, San Diego, CA.
Israelachvili, J.N., Tabor, D., 1972. Measurement of vanderwaals dispersion forces in range 1.5 to 130 nm. Proc. R. Soc. Lond. A 331, 19–38.
Kendall, K., 1975. Thin-film peeling – elastic term. J. Phys. D: Appl. Phys. 8, 1449–1452.
Kim, T.W., Bhushan, B., 2008. The adhesion model considering capillarity for gecko attachment system. J. R. Soc. Interface 5, 319–327.
Lee, J.H., Fearing, R.S., Komvopoulos, K., 2008. Directional adhesion of gecko-inspired angled microfiber arrays. Appl. Phys. Lett. 93, 191910.
Persson, B.N.J., 2003. On the mechanism of adhesion in biological systems. J. Chem. Phys. 118, 7614–7621.
Persson, B.N.J., Gorb, S., 2003. The effect of surface roughness on the adhesion of elastic plates with application to biological systems. J. Chem. Phys. 119, 11437–11444.
Pesika, Noshir S., Tian, Y., et al., 2007. Peel-zone model of tape peeling based on the gecko adhesive system. J. Adhes. 83, 383–401.
Rahulkumar, P., Jagota, A., Bennison, S.J., Saigal, S., 2000. Cohesive element modeling of viscoelastic fracture: application to peel testing of polymers. Int. J. Solids Struct. 37, 1873–1897.
Rose, J.H., Ferrante, J., Smith, J.R., 1981. Universal binding-energy curves for metals and bimetallic interfaces. Phys. Rev. Lett. 47, 675–678.
Russell, A.P., 1975. A contribution to the functional analysis of the foot of the Tokay, Gekko gecko (Reptilia, Gekkonidae). J. Zool. Lond. 176, 437–476.
Sitti, M., Fearing, R.S., 2003. Synthetic gecko foot-hair micro/nano-structures as dry adhesives. J. Adhes. Sci. Tehnol. 17, 1055–1073.
Sun, W.X., Neuzil, P., Kustandi, T.S., Oh, S., Samper, V.D., 2005. The nature of the gecko lizard adhesive force. Biophys. J. 89, L14–L17.
Thouless, M.D., Jensen, H.M., 1992. Elastic fracture mechanics of the peel-test geometry. J. Adhes. 38, 185–197.
Tian, Y., Pesika, N., Zeng, H.B., Rosenberg, K., Zhao, B.X., McGuiggan, P., Autumn, K., Israelachvili, J., 2006. Adhesion and friction in gecko toe attachment and detachment. Proc. Natl. Acad. Sci. USA 103, 19320–19325.
Tvergaard, V., Hutchinson, J.W., 1996. Effect of strain-dependent cohesive zone model on predictions of crack growth resistance. Int. J. Solids Struct. 33, 3297–3308.
Wei, Y.G., 2004. Modeling nonlinear peeling of ductile thin films-critical assessment of analytical bending models using FE simulations. Int. J. Solids Struct. 41, 5087–5104.
Willis, J.R., 1967. A comparison of fracture criteria of Griffith and Barenblatt. J. Mech. Phys. Solids. 15, 151–162.
Xu, X.P., Needleman, A., 1994. Numerical simulations of fast crack-growth in brittle solids. J. Mech. Phys. Solids. 42, 1397–1434.
Yao, H., Gao, H., 2006. Mechanics of robust and releasable adhesion in biology: bottom-up designed hierarchical structures of gecko. J. Mech. Phys. Solids. 54, 1120–1146.
Yuan, H., Chen, J.F., Teng, J.G., Lu, X.Z., 2007. Interfacial stress analysis of a thin plate bonded to a rigid substrate and subjected to inclined loading. Int. J. Solids Struct. 44, 5247–5271.
Zhao, B.X., Pesika, N., Rosenberg, K., Tian, Y., Zeng, H.B., McGuiggan, P., Autumn, K., Israelachvili, J., 2008. Adhesion and friction force coupling of gecko setal arrays: implications for structured adhesive surfaces. Langmuir 24, 1517–1524.